

Analysis of the UF₆-Xe Direct Nuclear-Pumped Laser

H. A. Hassan*

North Carolina State University, Raleigh, N. C.

The quenching role of UF₆ in noble gas nuclear-pumped lasers is examined. Detailed results are presented for the He-UF₆-Xe system. These results indicate that depletion of the atomic ion is the mechanism responsible for the observed behavior. Based on this, it is concluded that UF₆ is not compatible with noble gas lasers. In addition to identifying the quenching role of UF₆, some key rates whose rate constants are not known are identified.

Introduction

IF direct nuclear pumping is to become a viable pumping mechanism for high-power lasers, then a self-critical reactor using gaseous UF₆ must be constructed and a suitable lasing material found.¹ In such a reactor, pumping is achieved by the fission fragments from the ²³⁵U(n,ff)FF reaction. Experiments with reactor-excited lasers, using UF₆ as a volume source of fission fragments in Xe-Ar mixtures,² indicated that lasing is possible at 2.65 μm for a total pressure of about 600 Torr. However, quenching resulted when the partial pressure of UF₆ exceeded 1 Torr.

The object of this investigation is to study the kinetics of nuclear pumping of noble gases by the ²³⁵U(n,ff)FF reaction and to deduce from that the quenching role of UF₆. Although the experiment employed an Ar-Xe-UF₆ mixture, detailed calculations are carried for a He-Xe-UF₆ mixture. This is because more kinetic data are available for He; moreover, the pumping mechanism is not expected to depend on the buffer gas as long as it is a noble gas with ionization and excitation potentials higher than those for Xe. It will be assumed that He is the dominant substance in the system and, as such, is initially excited and ionized by fission fragments. The energy stored in the excited and ionized states of He is then transferred to the lasing material by charge transfer and Penning ionization. For noble gas lasers,^{3,4} recombination of the atomic ion yields the upper laser level, while recombination of the molecular ion yields the lower laser level. Thus, there is an optimum noble gas concentration for which the power output is maximum.

Two possible mechanisms may be advanced for interpreting the termination of lasing observed in the experiments of Ref. 2. The first assumes that electron attachment is the dominant mechanism, while the second is based on the depletion of the atomic ion as a result of neutralization of Xe⁺ by UF₆⁻ and F⁻. The calculations indicate that the mechanism depends, to a large extent, on the neutralization rate of UF₆⁺ and UF₆⁻ for which no measurements are available. For the case where the neutralization rate is comparable to rates involving complex ions,⁵ the results were not consistent with available experiment. However, when lower rates were assumed, the results were consistent with the observation of Ref. 2. Calculations using the lower rate indicate that depletion of the atomic ion is the mechanism responsible for quenching.

Analytical Formulation

A typical experimental setup of a nuclear-pumped laser consists of a tube filled with fissionable material and a lasing

medium surrounded by a moderator and placed in a fast-burst reactor.³ The high-energy fission fragments, resulting from the interaction of thermal neutrons with the fissionable material, together with the primary and secondary electrons, ionize and excite the background gas. It is generally assumed that the fission fragments resulting from the ²³⁵U(n,ff)FF reaction fall into two groups: a light group with an average mass number of 96, an average charge of 20 e, and an average initial energy of 98 MeV; and a heavy group with an average mass number of 140, an average charge of 22 e, and an average initial energy of 67 MeV. Using this information, Wilson and De Young⁶ derived the following approximate expression for the power density (w/cm³) released by the ²³⁵U(n,ff)FF reaction in representative laser tubes at pressures of the order of 1 atm:

$$P_d \approx 4.2 \times 10^{-16} \frac{\alpha(1-\alpha)p\phi_0}{1-\alpha+\beta\alpha} \quad (1)$$

where α is the UF₆ concentration, p the pressure in atmospheres, ϕ_0 the neutron flux, and β the ratio of the range of fission fragments in He to that in UF₆.

The analysis employed here follows closely that employed in Ref. 7. Thus, particles in different excited states are treated as different species and the multifluid conservation equations are used to describe the resulting plasma. It is shown in Ref. 7 that, for typical laser experiments, the pressure and temperature are essentially constant and the composition is obtained from the relation

$$R_s = 0 \quad (2)$$

where R_s is the production rate of species s resulting from nuclear and kinetic processes. Expressions for R_s follow from the important kinetic processes in the UF₆-He-Xe system and the rates of ionization and excitation of He. The latter follow from Eq. (1) and the appropriate w values, i. e., the energy required to create an excited or an ionized state.

Because we are interested in determining which Xe lines are capable of lasing, all 6s, 6p, and 5d states of Xe are considered together with the atomic and molecular ions. UF₆ is allowed to dissociate resulting in the formation of F, F⁻, F₂, UF₆⁻, UF₆⁺, UF₅, UF₅⁻, UF₄⁺, and UF₄. All He excited states are lumped in a single state. The above, together with the electrons, the atomic and molecular helium ions, and the ground states of He, Xe, and UF₆ result in a system consisting of 34 different species. Excimers were not included in this investigation.

Hundreds of reactions involving the above constituents can take place in an UF₆-He-Xe system. However, because of the lack of rate data, especially those involving UF₆ and its dissociation products, only 110 simultaneous reactions are considered. As indicated previously, it is assumed that the power deposited generate ionized and excited states of He.

Received Jan. 11, 1980; presented as Paper 80-0095 at the AIAA 18th Aerospace Sciences Meeting, Pasadena, Calif., Jan 14-16, 1980; revision received May 5, 1980. Copyright © American Institute of Aeronautics and Astronautics, Inc., 1980. All rights reserved.

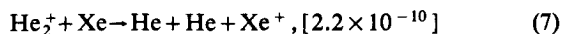
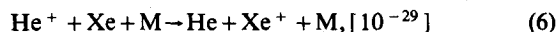
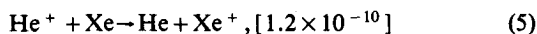
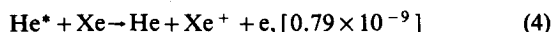
Index categories: Lasers; Nuclear Fission.

*Professor of Mechanical and Aerospace Engineering. Associate Fellow AIAA.

Because of the high pressures of interest, He⁺ is converted into He₂⁺ according to the reaction



with a rate⁸ ranging from 6.78×10^{-32} to 10.7×10^{-32} cm⁶/s. Both Xe and UF₆ have ionization potentials lower than the ionization and excitation potentials of He. Thus, energy is transferred from helium to Xe and UF₆ by charge transfer and Penning ionization. As a result, Xe⁺ is formed according to the reactions^{5,9,10}



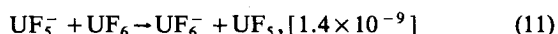
with M being a third body and quantities in square brackets indicating rate constants.

The situation involving UF₆ is not clear. In general, charge transfer reactions involving ions with large recombination energies and polyatomic molecules tend to produce mainly dissociative ion products. On the other hand, dimer ions have somewhat lower recombination energies and thus do not cause as much dissociative ionization. Thus, reactions involving He products and UF₆ are taken as

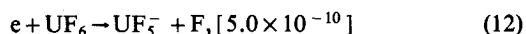


In the absence of direct measurements, the above rates are estimates taken from Ref. 5.

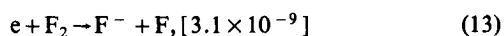
Electron attachment resulting in the formation of UF₆⁻ is characterized by a rather low attachment rate.¹¹ Thus, it is generally believed that the formation of UF₆⁻ follows from the charge transfer reaction¹²



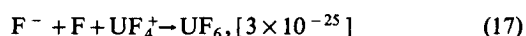
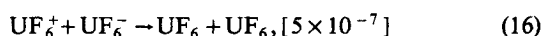
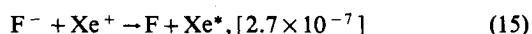
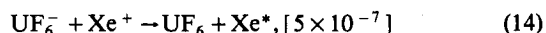
with UF₅⁻ being formed according to the reaction¹¹



The rate indicated for the above reaction is that for thermal electrons with higher rates being observed for more energetic electrons. Another negative ion is formed by the dissociative detachment reaction¹³



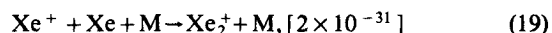
With the presence of negative and positive ions in the system, the following mutual neutralization reactions are considered.



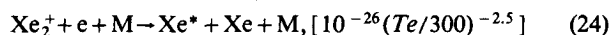
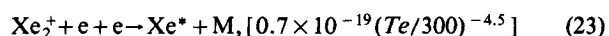
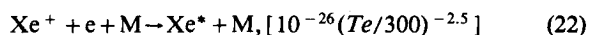
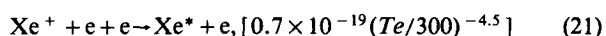
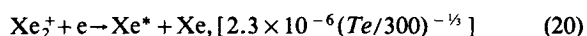
The above rates are estimates based on the summary presented in Chap. 24 of Ref. 5. Because the electron af-

finities of UF₆ and F are about 4.9 and 3.6 eV, respectively, the Xe* in reactions (14) and (15) has, on the average, an energy lower than the lower laser level. Because of this, Xe* in reactions (14) and (15) was taken as the ground state. As previously indicated, a series of rates for reaction (18) were employed ranging from 5×10^{-7} to 5×10^{-10} .

Just as helium atomic ions are converted into molecular ions, xenon molecular ions are formed according to the reaction¹⁴



Recombination of the molecular and atomic Xe ions dictate which laser transition is possible. Although the overall rates are known, the recombination products are not. The rates for the various recombination processes involving xenon can be summarized as follows^{15,5}:

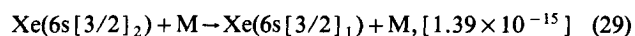
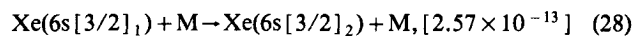
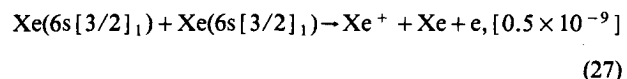
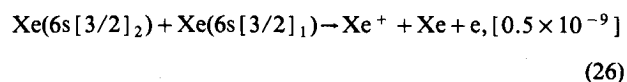
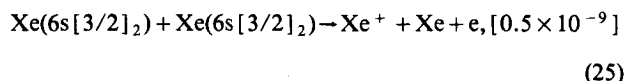


The two-body recombination reaction, Eq. (20), was studied by Shui et al.,¹⁵ who measured the intensities of various lines in a recombining helium-xenon afterglow. A number of lines of interest could not be examined because of equipment limitations, but the intensities of lines involving 6p states were measured. For a plasma state where recombination and spontaneous emission are the dominant loss and production mechanisms, the total production rate is equal to the loss rate for a particular transition divided by the branching ratio for that transition. Given the intensities of several lines involving different states, one can then determine the relative production rates for these states. Using the intensity data of Ref. 15 and assuming that Xe₂⁺ recombination produces p states only, the fractions of the total recombination rate populating the various states were established as follows: 6p[5/2]₃, 0.40; 6p[3/2]₂, 0.22; 6p[1/2]₀, 0.17; 6p[3/2]₁, 0.12; 6p[5/2]₂, 0.03; and 6p[1/2]₁, 0.03. In the absence of other measurements, similar fractions were employed in other reactions involving Xe₂⁺ recombination.

Data involving Xe⁺ recombination are nonexistent. Therefore, it is assumed in this study that the products of Xe⁺ recombination are evenly distributed over 6p and 5d states. Obviously, other choices would yield different results.

Spontaneous emission reactions are important loss and production mechanisms for the noble gas-excited states. All transitions involving 6p and 5d states were incorporated in this work and their rates were taken from Ref. 16.

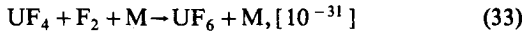
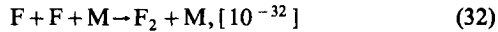
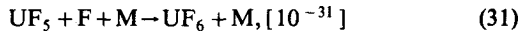
The final Xe states that require consideration are the 6s states. Reactions involving these states are taken as follows:





Rates of reactions (25-27) were estimated from Ref. 17, while those for reactions (28-30) were taken from Ref. 18.

The final rates employed in this model involved the recombination of fluorine and UF_6 dissociation products



The above rates were estimated from Ref. 5.

The solution of the kinetic model gives the number densities of the species present in the plasma. Knowing the number densities, one can calculate the gain coefficient $\gamma(\nu)$ for the various transitions⁷

$$\gamma_{mn} = \frac{c^2 g_m}{8\pi \nu^2} A_{mn} \left[\frac{N_m}{g_m} - \frac{N_n}{g_n} \right] G(\nu) \quad (34)$$

where $G(\nu)$ is the shape factor, N_m and N_n are the number densities of the upper and lower levels, g the degeneracy, A_{mn} the Einstein coefficient for spontaneous transitions from level m to level n , c the speed of light, and ν the frequency. The shape factor is affected by both Doppler and pressure broadening. For pressures of interest here, pressure broadening is the dominant effect and, therefore,

$$G = \frac{2}{\pi} \sum_t \nu_{st} \quad (35)$$

where

$$\nu_{st} = \frac{2}{3} \left[2k \left(\frac{1}{m_s} + \frac{1}{m_t} \right) \right]^{1/2} Z_{st} N_t \quad (36)$$

k is the Boltzmann constant, Z_{st} the collision cross section, s the lasing gas, and t represents other gases in the system. The collision cross sections were calculated assuming a Lennard-Jones potential.¹⁹

Results and Discussion

Small signal gain coefficients were calculated for various mixtures and pressures and a flux of 3×10^{16} neutrons/cm², which is representative of fast burst reactors. No attempt was made to study the effects of neutron flux on gain coefficient because previous work^{4,20} has indicated that the relationship is almost linear. Unless indicated otherwise, the pressure is 1 atm. The electron temperature T_e is assumed to be 300 K.

Experiments involving pumping of Ar-Xe mixtures by the $^{235}\text{U}(\text{n,ff})\text{FF}$ reaction² indicate that quenching takes place when the UF_6 fraction exceeds 1 in 600. Thus, if the kinetic model is consistent with experiment, one should expect that the gain coefficient will decrease with increasing UF_6 concentration. In an attempt to calculate the small signal gain coefficient, it became evident that it is rather sensitive to the neutralization reaction involving UF_6^- and UF_4^+ ; a reaction whose rate is not known. Because of this, a parametric study involving the neutralization rate of UF_6^- and UF_4^+ was undertaken. Figure 1 shows the gain coefficient for the $3.99 \mu\text{m}$ line (the line with the highest gain coefficient for the range of parameters investigated) as a function of UF_6 fraction for a rate coefficient of 5×10^{-7} , which is representative of neutralization of complex ions,⁵ while Fig. 2 represents a similar plot for a rate coefficient of 5×10^{-10} . As seen from Fig. 1, the gain coefficient increases with UF_6 fractions exceeding

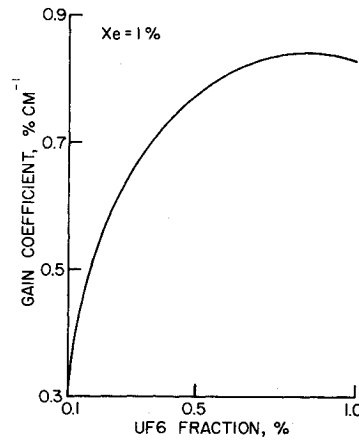


Fig. 1 Effect of UF_6 concentration of gain [high rate for reaction (18)].

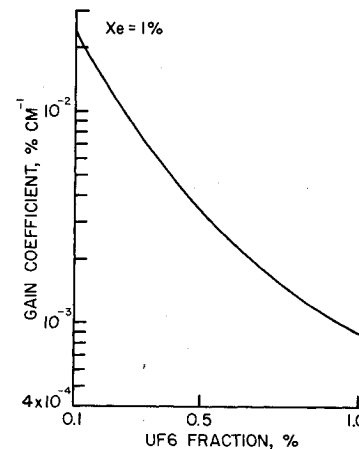


Fig. 2 Effect of UF_6 concentration on gain.

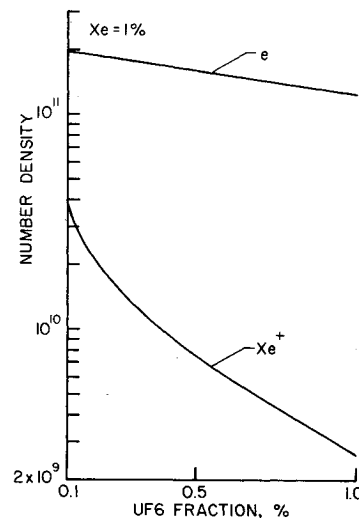


Fig. 3 Effect of UF_6 concentration on electron and Xe^+ number densities.

1/600; the fraction above which quenching took place.² This indicates that the neutralization rate coefficient for UF_4^+ and UF_6^- employed in generating Fig. 1 is unrealistic. On the other hand, for a neutralization rate coefficient of 5×10^{-10} , the gain coefficient decreases with UF_6 fraction in agreement with experimentally observed trends. Because of this, the neutralization rate for UF_6^- and UF_4^+ is taken as 5×10^{-10} , and the following results are based on this rate.

There are two possible explanations for laser quenching with increased UF_6 concentration. The first is based on increased electron attachment with the result that fewer electrons will be available for recombination with Xe^+ . Such a mechanism will manifest itself by a decreased electron density with an increased UF_6 concentration. The other explanation

Table 1 Gain coefficients

Transition	λ , μm	γ , $\% \text{cm}^{-1}$
$5d[1/2]_0 - 6p[1/2]_1$	3.99	0.241×10^{-1}
$5d[1/2]_1 - 6p[1/2]_1$	3.68	0.606×10^{-2}
$5d[1/2]_1 - 6p[3/2]_1$	12.27	0.75×10^{-3}
$5d[1/2]_1 - 6p[5/2]_2$	5.36	0.125×10^{-2}

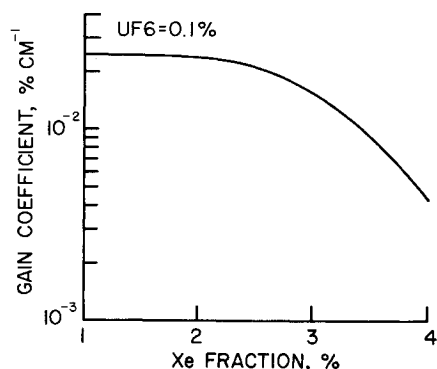


Fig. 4 Influence of xenon concentration on gain.

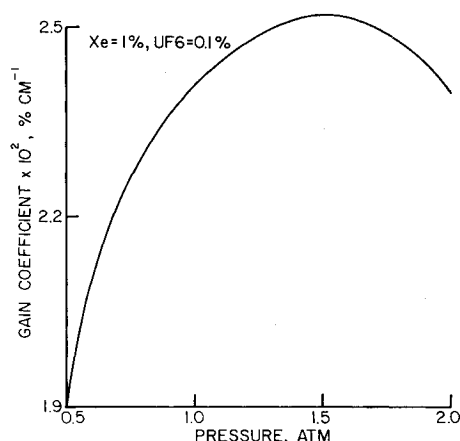


Fig. 5 Influence of pressure on gain.

involves the depletion of the atomic ion by recombination with F^- and UF_6^- . This, in turn, results in a decrease in the number density of the upper laser level. Plots of the number densities of electrons and Xe^+ as a function of UF_6 concentration are shown in Fig. 3. Figure 3 indicates rather clearly that the second mechanism is the one responsible for laser quenching.

The model incorporates all d and p states and thus is capable of predicting all possible d to p transitions. Table 1 shows a listing of all transitions that exhibited positive gain at a pressure of 1 atm and Xe and UF_6 fractions of 1 and 0.1%. The experiments of Ref. 2 indicated lasing on the $2.65 \mu\text{m}$ line, while the present analysis indicates that lasing should have taken place on the $3.99 \mu\text{m}$ line. This discrepancy is a result of the assumption that the products of Xe^+ recombination are evenly distributed over $6p$ and $5d$ states. Had we assumed that Xe^+ recombination resulted in the preferential pumping of the $5d[3/2]_1$ state, we would have predicted lasing on the $2.65 \mu\text{m}$ line. Because the $3.99 \mu\text{m}$ line is the only line that showed measurable gain for Xe concentration less than 4% and UF_6 concentrations less than 1%, the following discussion will be devoted to this line.

For a given pressure and Xe fraction, there is an optimum UF_6 concentration for optimum gain. This is because power

deposition is proportional to UF_6 concentration. On the other hand, depletion of Xe^+ increases with UF_6 concentration. These two competing effects point to the existence of an optimum UF_6 concentration. Similarly, because Xe_2^+ increases with increased Xe concentration and because Xe_2^+ recombination yields the lower laser level, there is an optimum Xe fraction for a given power deposition and pressure. These considerations are responsible for the behavior indicated in Figs. 2 and 4.

Figure 5 shows the effect of pressure on the gain coefficient. Increasing the pressure results in an increase in Xe_2^+ and this results in an increase in the lower laser level. On the other hand, increasing the pressure results in more power deposition into the system. Thus, for a given mixture, there is an optimum pressure for optimum gain.

The results also indicate that optimum conditions are influenced by the rates employed in the model. This points to the need for reliable rate measurements involving UF_6 and its dissociation products. The same holds for the recombination products of Xe^+ and Xe_2^+ .

Conclusions

The present calculations indicate that depletion of the atomic ion is the mechanism responsible for the observed quenching of laser action in noble gas lasers with increasing UF_6 concentrations. Because of this, UF_6 is not compatible with noble gas lasers.

Acknowledgment

This work was supported in part by NASA Grant NSG 1058.

References

- Rodgers, R. J., "Initial Conceptual Design Study of Self-Critical Nuclear Pumped Laser Systems," NASA CR-3128, April 1979.
- De Young, R. J., "LaRC Results on Nuclear Pumped Rare Gas Lasers," in *Nuclear Pumped Lasers*, NASA Conf. Publ. 2107, 1979, pp. 45-60.
- De Young, R. J., Jalufka, N. W., and Hohl, F., "Direct Nuclear-Pumped Lasers Using the $^3\text{He}(n,p)^3\text{H}$ Reaction," *AIAA Journal*, Vol. 16, Sept. 1978, pp. 991-998.
- Deese, J. E. and Hassan, H. A., "Direct Nuclear Pumping by a Volume Source of Fission Fragments," *AIAA Journal*, Vol. 16, Oct. 1978, pp. 1030-1034.
- Bartner, M. H. and Baurer, T. (Eds.), *Defense Nuclear Agency Reaction Rate Handbook Series*, Dept. of Defense Information and Analysis Center, General Electric Co., Santa Barbara, Calif., 1972, Chaps. 16 and 24.
- Wilson, J. W. and De Young, R. J., "Power Deposition in Volumetric $^{235}\text{UF}_6$ -He Fission-Pumped Nuclear Lasers," *Journal of Applied Physics*, Vol. 49, March 1978, pp. 989-993.
- Deese, J. E. and Hassan, H. A., "Analysis of Nuclear Induced Plasmas," *AIAA Journal*, Vol. 14, Nov. 1976, pp. 1589-1597.
- Chen, C. H., Judish, J. P., and Payne, M. G., "Charge Transfer and Penning Ionization of N_2 , CO , CO_2 and H_2S in Proton Excited Helium Mixtures," *The Journal of Chemical Physics*, Vol. 67, Oct. 1977, pp. 3376-3381.
- Riola, J. P., Howard, J. S., Rundel, R. D., and Stebbings, R. F., "Chemionization Reactions Involving Metastable Helium Atoms," *Journal of Physics B: Atomic and Molecular Physics*, Vol. 7, Feb. 1974, pp. 376-385.
- Lee, F. W., Collins, C. B., and Waller, R. A., "Measurement of the Rate Coefficients for the Bimolecular and Termolecular Charge Transfer Reactions of He_2^+ with Ne, Ar, N_2 , CO , CO_2 and CH_4 ," *The Journal of Chemical Physics*, Vol. 65, Sept. 1976, pp. 1605-1615.
- Beauchamp, J. L., "Properties and Reactions of Uranium Hexafluoride by Ion Cyclotron Resonance Spectroscopy," *The Journal of Chemical Physics*, Vol. 64, Jan. 1976, pp. 718-723.
- Stockdale, J. A. D., Compton, R. N., and Schweinler, H. C., "Negative Ion Formation in Selected Hexafluoride Molecules," *The Journal of Chemical Physics*, Vol. 53, Aug. 1970, pp. 1502-1507.

¹³Sides, G. D., Tiernan, T. O., and Hanrahan, R. J., "Measurement of Thermal Electron Dissociative Attachment Rate Constants for Halogen Gases Using a Flowing Afterglow Technique," *The Journal of Chemical Physics*, Vol. 65, Sept. 1976, pp. 1966-1975.

¹⁴Vitols, A. P. and Oskam, H. J., "Reaction Rate Constant for $\text{Xe}^+ + 2\text{Xe} \rightarrow \text{Xe}_2^+ + \text{Xe}$," *Physical Review A*, Vol. 8, Oct. 1973, pp. 1860-1863.

¹⁵Shui, Y. J. and Biondi, M. A., "Dissociative Recombination in Argon: Dependence of the Total Rate Coefficient and Excited State Production with Electron Temperature," *Physical Review A*, Vol. 17, March 1978, pp. 868-872.

¹⁶McGuire, E. J., "Radiative Transition Rates in Atomic Xe," Sandia Labs. Rept. SAND 76-0196, May 1976.

¹⁷George, E. V. and Rhodes, C. K., "Kinetic Model of Ultraviolet Inversions in High Pressures Rare-Gas Plasmas," *Applied Physics Letters*, Vol. 23, Aug. 1973, pp. 139-141.

¹⁸Leichner, P. K., Palmer, K. F., Cook, J. D., and Thieneman, M., "Two- and Three-Body Collision Coefficients for Xe ($^3\text{P}_1$) and Xe ($^3\text{P}_2$) Atoms and Radiative Lifetime of the Xe_2 (1u) Molecule," *Physical Review A*, Vol. 13, May 1976, pp. 1787-1792.

¹⁹Hirschfelder, J. O., Curtis, C. P., and Bird, R. B., *Molecular Theory of Gases and Liquids*, 2nd ed., John Wiley and Sons, Inc., New York, 1964, pp. 1110-1111.

²⁰Hassan, H. A., "Kinetics of a CO Nuclear Pumped Laser," AIAA Paper 79-1566, July 1979.

From the AIAA Progress in Astronautics and Aeronautics Series...

ENTRY HEATING AND THERMAL PROTECTION—v. 69

HEAT TRANSFER, THERMAL CONTROL, AND HEAT PIPES—v. 70

Edited by Walter B. Olstad, NASA Headquarters

The era of space exploration and utilization that we are witnessing today could not have become reality without a host of evolutionary and even revolutionary advances in many technical areas. Thermophysics is certainly no exception. In fact, the interdisciplinary field of thermophysics plays a significant role in the life cycle of all space missions from launch, through operation in the space environment, to entry into the atmosphere of Earth or one of Earth's planetary neighbors. Thermal control has been and remains a prime design concern for all spacecraft. Although many noteworthy advances in thermal control technology can be cited, such as advanced thermal coatings, louvered space radiators, low-temperature phase-change material packages, heat pipes and thermal diodes, and computational thermal analysis techniques, new and more challenging problems continue to arise. The prospects are for increased, not diminished, demands on the skill and ingenuity of the thermal control engineer and for continued advancement in those fundamental discipline areas upon which he relies. It is hoped that these volumes will be useful references for those working in these fields who may wish to bring themselves up-to-date in the applications to spacecraft and a guide and inspiration to those who, in the future, will be faced with new and, as yet, unknown design challenges.

Volume 69—361 pp., 6 × 9, illus., \$22.00 Mem., \$37.50 List
Volume 70—393 pp., 6 × 9, illus., \$22.00 Mem., \$37.50 List

TO ORDER WRITE: Publications Dept., AIAA, 1290 Avenue of the Americas, New York, N.Y. 10104